

Relative positions of the 2Δ peaks in Raman and tunneling spectra of d -wave superconductors

Andrey V. Chubukov, Nathan Gemelke, and Ar. Abanov

Department of Physics, University of Wisconsin, Madison, Wisconsin 53706

(Received 7 October 1999)

We study B_{1g} Raman intensity $R(\Omega)$ and the density of states $N(\omega)$ in isotropic two-dimensional d -wave superconductors. For an ideal gas, $R(\Omega)$ and $N(\omega)$ have sharp peaks at $\Omega = 2\Delta$ and $\omega = \Delta$, respectively, where Δ is the maximum value of the gap. We study how the peak positions are affected by the fermionic damping due to impurity scattering. We show that while the damping generally shifts the peak positions to larger frequencies, the peak in $R(\Omega)$ still occurs at almost twice the peak position in $N(\omega)$ and therefore cannot account for the experimentally observed downturn shift of the peak frequency in $R(\Omega)$ in underdoped cuprates compared to twice that in $N(\omega)$. We also discuss how the fermionic damping affects the dynamical spin susceptibility.

The unusual physical properties of cuprate superconductors have continued to be of high interest to condensed-matter physicists for more than a decade. In recent years, much attention was devoted to the study of collective bosonic excitations in the superconducting and pseudogap phases.¹⁻³ The most notable experimental observation is the discovery of the resonance mode in the dynamical spin susceptibility.^{1,2} This mode is centered at the antiferromagnetic momentum $Q = (\pi, \pi)$, and physically reflects the fact that near antiferromagnetic instability, collective spin excitations in a d -wave superconductor are undamped, propagating spin waves at energies smaller than 2Δ .⁴⁻⁸ Less attention is devoted to the study of possible resonance bosonic excitations at zero momentum transfer. These excitations are probed by Raman scattering which generally measures the imaginary part of the fully renormalized particle-hole susceptibility at vanishingly small incoming momentum, weighted with Raman form factors which depend on the scattering geometry.^{9,10} The experiments relevant to our discussion were performed in B_{1g} geometry where the Raman form factors are the largest for fermionic momenta near $(0, \pi)$ and symmetry related points where the $d_{x^2-y^2}$ gap $\Delta(k)$ is near its maximum Δ .^{11,12}

In a BCS theory for a d -wave superconductor, B_{1g} Raman intensity $R(\Omega)$ logarithmically diverges at 2Δ and rapidly, as ω^3 , decreases at smaller frequencies.¹² Experimental data for overdoped Bi2212 are qualitatively consistent with this behavior.^{3,13} Furthermore, the 2Δ extracted from $R(\Omega)$ is almost exactly twice the gap extracted from superconductor-insulator-normal metal junctions (SIN) tunneling data, which measure a single particle density of states (DOS) $N(\omega)$.¹⁴ With underdoping, however, the peak frequency in $R(\Omega)$ progressively deviates down from the 2Δ extracted from the tunneling experiments.³

Blumberg, Morr, and one of us (CBM) (Ref. 15) attributed this deviation to a final-state interaction between scattered quasiparticles. They argued that the magnetically mediated final-state interaction in B_{1g} geometry is attractive and gives rise to a pseudo-resonance in $R(\Omega)$ at a frequency Ω_{res} , which with underdoping progressively deviates down from 2Δ .

An alternative to the resonance mode scenario is one in which the final-state interaction is irrelevant, and the discrepancy between Raman and tunneling data is due to fermionic

incoherence, which generally shifts the positions of both the Raman peak and the peak in the DOS. In this paper, we show that the shifts in the peak positions of $R(\Omega)$ and $N(\omega)$ due to fermionic damping are *correlated* such that without final-state interaction, the peak in $R(\Omega)$ is still located at almost exactly twice the peak frequency in $N(\omega)$. This result implies that the experimentally observed relative downturn deviation of the peak in the Raman intensity *cannot* be explained by purely fermionic self-energy effects, and leaves the resonance mode scenario as the most probable one.

We begin with the general expressions for $R(\Omega)$ and $N(\omega)$ in a superconductor. The DOS is the imaginary part of the local normal quasiparticle Green's function, and the Raman intensity without final-state interaction is the imaginary part of the fermionic polarization bubble with a zero momentum transfer, weighted with Raman vertices.^{19,20} We have, up to an overall factor

$$R(\Omega) = \text{Im} \int dk d\omega V_{B_{1g}}^2(\mathbf{k}) (G_{sc}(k, \omega_+) G_{sc}(k, \omega_-) + F(k, \omega_+) F(k, \omega_-));$$

$$N(\omega) = \text{Im} \int dk G_{sc}(k, \omega). \quad (1)$$

Here, $V_{B_{1g}}(\mathbf{k}) \propto \cos k_x - \cos k_y$ is the B_{1g} Raman vertex, $\omega_{\pm} = \omega \pm \Omega/2$, and $G_{sc}(k, \omega)$ and $F(k, \omega)$ are normal and anomalous quasiparticle Green's functions given by

$$G_{sc}(k, \omega) = G_n^{-1}(-k, -\omega) / (G_n^{-1}(k, \omega) G_n^{-1}(-k, -\omega) + \Delta_k^2)$$

$$F(k, \omega) = i\Delta_k / (G_n^{-1}(k, \omega) G_n^{-1}(-k, -\omega) + \Delta_k^2). \quad (2)$$

Here, $G_n^{-1}(k, \omega) = \Sigma(\mathbf{k}, \omega) - \epsilon_k$, where $\Sigma(\mathbf{k}, \omega)$ is the fermionic self-energy (which also absorbs a bare ω term), and Δ_k is the superconducting gap, which for a $d_{x^2-y^2}$ superconductor behaves as $\Delta_k \propto \cos k_x - \cos k_y$.

In an ideal gas, the fermionic self-energy is absent (i.e., $\Sigma(\mathbf{k}, \omega) = \omega$). To simplify the discussion, we assume that the Fermi surface is circular, for which both $R(\Omega)$ and $N(\omega)$ can be evaluated exactly.¹³ Substituting the momentum inte-

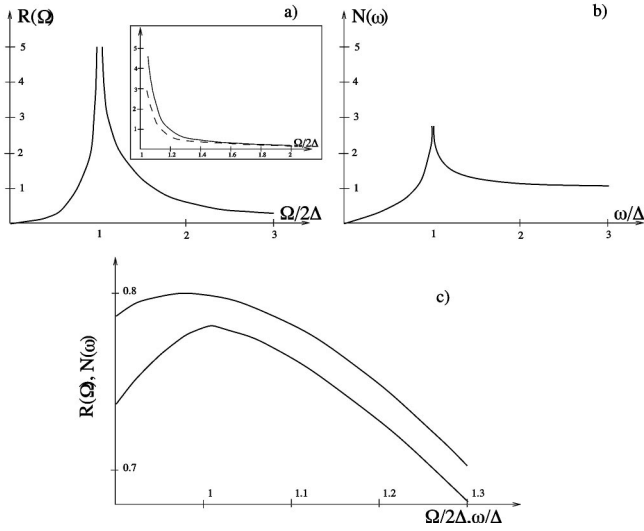


FIG. 1. The behavior of the Raman intensity $R(\Omega)$ and the DOS $N(\omega)$ in d -wave superconductors (a). (b) Fermi-gas results ($\gamma = 0$) Solid lines: d -wave results, dashed lines: s -wave results shown for comparison. The inset shows the behavior of $R(\Omega)$ close to the threshold frequency 2Δ . (c) The results for $\gamma = 0.2\Delta$ [Eq. (8)] The normalized frequencies are $\bar{\omega} = \omega/\Delta$ and $\bar{\Omega} = \Omega/(2\Delta)$. Observe that for d -wave superconductors, the peak in the Raman intensity is located at larger normalized frequency than the peak in the density of states.

gration by integration over $d\epsilon_k$, and approximating the k dependences of $V_{B_{1g}}(\mathbf{k})$ and Δ_k by $\cos \Theta$, one obtains for $\bar{\Omega}$, $\bar{\omega} < 1$ (Ref. 13)

$$R(\bar{\Omega}) = \frac{3\pi}{16} \bar{\Omega}^3 F\left(\frac{1}{2}, \frac{5}{2}, 3, \bar{\Omega}^2\right), \quad N(\bar{\omega}) = \frac{2}{\pi} \bar{\omega} K(\bar{\omega}), \quad (3)$$

and for $\bar{\Omega}$, $\bar{\omega} > 1$

$$R(\bar{\Omega}) = \frac{3\pi}{16\bar{\Omega}^2} F\left(\frac{1}{2}, \frac{5}{2}, 3, \frac{1}{\bar{\Omega}^2}\right), \quad N(\bar{\omega}) = \frac{2}{\pi} K\left(\frac{1}{\bar{\omega}}\right), \quad (4)$$

where $\bar{\omega} = \omega/\Delta$, $\bar{\Omega} = \Omega/(2\Delta)$, and $F(a, b, c, x)$ and $K(x)$ are hypergeometric and elliptical functions, respectively. The results for $R(\Omega)$ and $N(\omega)$ are plotted in Fig. 1(a) and (b). At the smallest frequencies, $R(\Omega) \propto \Omega^3$ and $N(\omega) \propto \omega$. At larger frequencies, the Raman intensity and the DOS diverge logarithmically at $\omega = \Delta$ and $\Omega = 2\Delta$, respectively. At even larger frequencies, the momentum dependence of the gap progressively becomes less relevant, and both $R(\Omega)$ and $N(\omega)$ acquire the same forms as in s -wave superconductors: $R(\bar{\Omega}) \propto 1/(\bar{\Omega} \sqrt{\bar{\Omega}^2 - 1})$, $N(\bar{\omega}) = \bar{\omega}/\sqrt{\bar{\omega}^2 - 1}$. Observe that $R(\Omega)$ crosses over to the s -wave behavior immediately above 2Δ . [see inset in Fig. 1(a)].

Our goal is to study how the peak positions and, more generally, the functional forms of $R(\Omega)$ and $N(\omega)$ are affected by the fermionic self-energy. In general, the fermionic self-energy comes from various sources, and at least part of it, associated with the scattering by the same bosonic excitations which give rise to superconductivity, has to be determined fully self-consistently from the Eliashberg-type equations.⁷ In this paper, we assume for simplicity that the

primary source for the fermionic damping is impurity scattering. We consider the fermionic self-energy in the self-consistent T -matrix formalism^{16,17} and neglect subtle two-dimensional (2D) effects beyond T -matrix approximation.¹⁸ Hirshfeld, Wolfe, and Einzel¹⁶ demonstrated that for a d -wave superconductor with a particle-hole symmetry and k -independent scattering potential, $\Sigma(k, \omega) = \omega + i\gamma_{|\omega} \text{sign}(\omega)$, where $\gamma_{|\omega}$ is a solution of the self-consistent equation^{16,17}

$$\gamma_{|\omega} = \gamma \frac{g_0(|\omega|)}{c^2 + g_0^2(|\omega|)}. \quad (5)$$

Here, γ is proportional to the impurity concentration, c is the cotangent of the scattering phase shift, and $g_0(|\omega|) = (i/\pi N_F) \Sigma_k G_{sc}(k, \omega) \text{sign}(\omega)$, where N_F is the normal-state DOS at the Fermi surface. The self-consistency of Eq. (5) is in the fact that $G_{sc}(k, \omega)$ given by formula (2) by itself depends on $\gamma(\omega)$ through $\Sigma(\omega)$. Physically this means that the fermionic self-energy due to impurity scattering is by itself affected by a superconductivity.

For a circular Fermi surface, the momentum integral over $G(k, \omega)$ can be performed exactly and yields $g_0(|\omega|) = (2/\pi) K(\Delta^2/\Sigma^2(\omega))$. In the normal state, $g_0(\omega) = 1$, and $\gamma_{|\omega}$ reduces to a constant $\gamma_{|\omega} = \gamma/(1+c^2)$. In a superconducting state, however, $\gamma_{|\omega}$ is complex and frequency dependent. Still, one can easily demonstrate that $\gamma_{|\omega}$ remains finite for all frequencies. Below we will need γ_0 and γ_Δ . For unitary scattering ($c=0$), we solved Eq. (5) at these frequencies and for $\gamma \ll \Delta$ obtained with logarithmical accuracy $\gamma_\Delta = (2/\pi) \gamma \log(\Delta/\gamma)$ and $\gamma_0 = (\pi \gamma \Delta / \log(\Delta/\gamma))^{1/2}$.

We now proceed with the calculations of the DOS and Raman intensity. As the self-energy is k independent, we can use the same trick as in earlier studies,^{8,15,21} and first integrate over momenta in Eq. (1). Substituting the momentum integration by the integration over ϵ_k and evaluating the integrals, we obtain¹⁵

$$N(\omega) = \text{Im} \int_0^{\pi/2} d\Theta \frac{\Sigma(\omega)}{D(\omega)}; \quad (6)$$

$$R(\Omega) = -\text{Re} \int_0^{\pi/2} d\Theta \cos^2 \Theta \times \int_{-\infty}^{\infty} d\omega \frac{(\Sigma_+ - \Sigma_-)^2 + (D_+ - D_-)^2}{4D_+ D_- (D_+ + D_-)}.$$

Here, $\omega_\pm = \omega \pm \Omega/2$, $\Sigma_\pm = \Sigma(\omega_\pm)$, $D_\pm = D(\omega_\pm)$, and $D(\omega) = \sqrt{\Delta^2 \cos^2 \Theta - \Sigma^2(\omega)}$.

As a warm up, consider the limit of small frequencies. Substituting $\Sigma(\omega) = \omega + i\gamma_0 \text{sign}(\omega)$ into Eq. (6) and expanding in frequency, we obtained

$$R(\bar{\Omega}) = \bar{\Omega} \bar{\gamma}_0^2 \log 1/\bar{\gamma}_0 + O(\bar{\Omega}^3);$$

$N(\bar{\omega})$

$$= N(0) + \bar{\omega} \left(1 - \frac{2}{\pi} \tan^{-1} \frac{\bar{\gamma}_0}{\bar{\omega}} \right) - \frac{2\bar{\gamma}_0}{\pi} \log \sqrt{1 + \left(\frac{\bar{\omega}}{\bar{\gamma}_0} \right)^2}, \quad (7)$$

where $N(0) = (2/\pi)\bar{\gamma}_0 \log 1/\bar{\gamma}_0$, and $\bar{\gamma}_0 = \gamma_0/\Delta$. At $\bar{\omega} \ll 1$, $N(\bar{\omega}) = N(0) + \bar{\omega}^2/(\pi\bar{\gamma}_0)$.

We see that fermionic damping (i) yields a linear frequency dependence of $R(\Omega)$, and (ii) yields a finite DOS at zero frequency, and the quadratic frequency dependence of $N(\bar{\omega})$ above $N(0)$. Both of these results agree with earlier studies.^{16,17}

We now consider $R(\Omega)$ and at $\Omega \approx 2\Delta$ and $\omega \approx \Delta$, where the Raman intensity and the DOS diverge in a Fermi gas. The Raman intensity near 2Δ has been previously evaluated numerically.¹⁷ We present the analytical results which allow us to compare the peak positions in $R(\omega)$ and $N(\omega)$.

Simple estimates show that near 2Δ , the integral in $R(\Omega)$ is dominated by $D_{\pm} \ll 1$, i.e., $\omega_{\pm} \approx \pm\Delta$. Substituting $\Sigma(\omega \approx \Delta) = \omega + i\gamma_{\Delta} \text{sign}(\omega)$ into Eq. (6) and expanding the integrands to first order in $\Omega - 2\Delta$ and $\omega - \Delta$, respectively, we obtain after lengthy but straightforward calculations

$$R(\bar{\Omega}) = \frac{\pi}{4\sqrt{2}} \text{Re} \left[\frac{F\left(\frac{1}{2}, \frac{1}{2}, 2, \frac{-2}{\bar{\Omega}-1+i\bar{\gamma}_{\Delta}}\right)}{\sqrt{\bar{\Omega}-1+i\bar{\gamma}_{\Delta}}}\right];$$

$$N(\bar{\omega}) = \frac{\sqrt{2}}{\pi} \text{Re} \left[\frac{K\left(i\sqrt{\frac{2}{\bar{\omega}-1+i\bar{\gamma}_{\Delta}}}\right)}{\sqrt{\bar{\omega}-1+i\bar{\gamma}_{\Delta}}}\right]. \quad (8)$$

Here $\bar{\gamma}_{\Delta} = \gamma_{\Delta}/\Delta$.

We now analyze these results. Near $\bar{\Omega} = \bar{\omega} = 1$, we find from Eq. (8) $R(\bar{\Omega}) \approx (-1/8)\log[(\bar{\Omega}-1)^2 + \bar{\gamma}_{\Delta}^2]$, $N(\bar{\omega}) \approx (-1/4\pi)\log[(\bar{\omega}-1)^2 + \bar{\gamma}_{\Delta}^2]$. We see that the logarithmical divergencies are cut by the fermionic damping, but, to a logarithmical accuracy, the peaks remain at the same positions as in a Fermi gas. In other words, fermionic damping gives rise to a broadening of the peaks in the Raman intensity and the DOS, but still, the peak in $R(\Omega)$ is located at twice the peak frequency of the DOS.

Calculations beyond the logarithmical accuracy show that the peak positions do shift to higher frequencies but the relative shift is opposite to the one detected in the experiments: the peak in $R(\bar{\Omega})$ shifts to higher frequencies for arbitrary γ_{Δ} ($\bar{\Omega}_{peak} - 1 \propto \bar{\gamma}_{\Delta}^2$ for $\bar{\gamma}_{\Delta} \ll 1$), while the peak in $N(\bar{\omega})$ shifts to high frequencies only if the damping exceeds a threshold value of $\bar{\gamma}_{\Delta} \approx 0.77$. Obviously, the magnitude of the shift in $N(\omega)$ is smaller than that in $R(\Omega)$. This behavior is illustrated in Fig. 1(c).

Note in passing that for s -wave superconductors, the same calculations which lead to Eq. (8) yield

$$R(x), N(x) \sim \left(\frac{\sqrt{1 + \alpha_x^2 + \alpha_x}}{(1 + \alpha_x^2)\bar{\gamma}_{\Delta}} \right)^{1/2}, \quad (9)$$

where $\alpha_x = (x-1)/(\bar{\gamma}_{\Delta})$ and $x = \bar{\Omega}$ for $R(x)$ and $x = \bar{\omega}$ for $N(x)$. Again, the divergencies at $\bar{\Omega} = \bar{\omega} = 1$ are gone and

substituted by the peaks at higher frequencies for which $\alpha_x = 1/2\sqrt{3}$. At the same time, the functional forms of $R(\bar{\Omega})$ and $N(\bar{\omega})$ are *identical*. This implies that in a dirty s -wave superconductor, the peak in the Raman intensity is also located exactly at twice the peak frequency in $N(\omega)$, though both peak positions shift from the Fermi gas values.

For completeness, we also discuss how fermionic damping affects the spin-polarization operator at the antiferromagnetic momentum Q . The form of this polarization operator is relevant for the interpretation of neutron-scattering and angle-resolved photoemission spectroscopy data.^{6,7,21}

The spin-polarization operator is related to the dynamical structure factor as $S_Q(\bar{\Omega}) \propto \text{Im}(\xi^{-2} - \Pi_Q(\bar{\Omega}))^{-1}$, where ξ is the magnetic correlation length.⁷ It is formally given by the same set of particle-hole bubbles made of normal and anomalous Green's functions as the Raman intensity, but differs from $R(\Omega)$ in two aspects. First, the antiferromagnetic spin polarization is a finite momentum probe, and the contribution to low-frequency $\text{Im}\Pi_Q(\Omega)$ only comes from the momentum range in the Brillouin zone where both particles in the bubble are near the Fermi-surface hot spots. Near hot spots, the superconducting gap is finite and close to Δ . In other words, the regions near the nodes of the $d_{x^2-y^2}$ gap do not contribute to the dynamical spin susceptibility near Q . Second, the vertices for $\Pi_Q(\Omega)$ contain Pauli matrices. For the anomalous FF term, the summation over spin projections yields an extra factor -1 compared to the Raman bubble. Performing the momentum integration in the GG and FF bubbles in the same way as before, and using the fact that $\Delta_k \Delta_{k+Q} = -\Delta^2$, we obtain⁷

$$\Pi_Q(\Omega) = i \int_{-\infty}^{\infty} d\omega \frac{\Sigma_+ \Sigma_- + D_+ D_- - \Delta^2}{2D_+ D_-}. \quad (10)$$

The overall factor is chosen such that in the normal state, $\Pi_Q(\Omega) = i|\omega|$.

For an ideal gas, the frequency integration in Eq. (10) yields $\text{Im}\Pi_Q(\bar{\Omega}) = 0$ and $\text{Re}\Pi_Q(\bar{\Omega}) \propto \bar{\Omega}^2$ at $\bar{\Omega} = \Omega/(2\Delta) < 1$. For large enough ξ , this behavior of $\Pi_Q(\Omega)$ gives rise to a resonant peak in $S_Q(\bar{\Omega})$ at a frequency where $\text{Re}\Pi_Q(\Omega) = \xi^{-2}$.^{5,8} At $\bar{\Omega} = 1$, $\text{Im}\Pi_Q(\Omega)$ jumps to a finite value, and $\text{Re}\Pi_Q(\Omega)$ diverges logarithmically.⁴ This behavior is shown in Fig. 2(a).

Substituting $\Sigma(|\omega| \approx \Delta)$ into Eq. (10) and performing the same calculations as before, we obtain near $\bar{\Omega} = 1$ and to first order in $\bar{\gamma}_{\Delta}$

$$\text{Im}\Pi_Q(\bar{\Omega}) = \frac{\Delta\pi}{2} \left(1 + \frac{2}{\pi} \arcsin \frac{\alpha_{\bar{\Omega}}}{\sqrt{\alpha_{\bar{\Omega}}^2 + 1}} \right)$$

$$\text{Re}\Pi_Q(\bar{\Omega}) = \Delta \left(\log \frac{1}{\bar{\gamma}_{\Delta}} - \Psi(\alpha_{\bar{\Omega}}) \right), \quad (11)$$

where, as before, $\alpha_{\bar{\Omega}} = (\bar{\Omega}-1)/(\bar{\gamma}_{\Delta})$, and in the limits of small and large α , $\Psi(\alpha)$ behaves as $\Psi(\alpha \ll 1) = \alpha^2/2$, and $\Psi(|\alpha| \rightarrow \infty) = \log|\alpha|$.

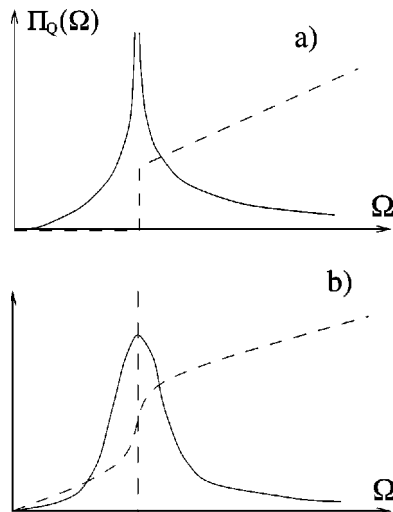


FIG. 2. The behavior of the spin polarization operator in the Fermi gas (a) and at a finite γ (b). Solid line: $\text{Re } \Pi_Q(\Omega)$, dashed line: $\text{Im } \Pi_Q(\Omega)$.

We see, similar to what we found for the Raman intensity and the DOS, the inclusion of the fermionic damping eliminates the singularities in the spin-polarization operator: $\text{Im } \Pi_Q$ changes continuously through $\bar{\Omega} = 1$, and $\text{Re } \Pi_Q$ is peaked but does not diverge at $\bar{\Omega} = 1$ (to first order in $\bar{\gamma}_\Delta$, the peak does not shift to higher frequencies). This behavior is shown in Fig. 2(b).

At small frequencies, the expansion in $\bar{\Omega}$ in Eq. (10) yields

$$\Pi_Q(\bar{\Omega}) = \frac{\pi}{2} \bar{\Omega}^2 + 2i \bar{\gamma}_0^2 |\bar{\Omega}|. \quad (12)$$

Again, similar to the result for $R(\Omega)$, the inclusion of a finite fermionic damping yields a nonzero $\text{Im } \Pi_Q(\Omega)$ down to the lowest frequencies. This result implies that in the presence of impurity scattering, the resonance peak in $S_Q(\Omega)$ has a finite width. This effect may account for the width of the resonance neutron peak near optimal doping. We, however, do not believe that fermionic damping is responsible for the increase of the peak width with underdoping—this last effect is likely to be caused by the frequency dependence of Δ associated with the pseudogap effects, which we do not consider here.²²

To summarize, we have considered in this paper a simple model form of the electronic damping and analyzed how it affects the forms of the Raman intensity, the DOS, and the spin-polarization operator at the antiferromagnetic momentum. We found that a finite damping eliminates artificial divergencies found in a Fermi gas consideration. Still, however, without final-state interaction, the peak in $R(\Omega)$ occurs at or beyond twice the peak frequency for the DOS, in contradiction with the experimental observations. This negative result implies that fermionic damping alone cannot account for the data, and supports the explanation of the downturn shift of the Raman peak with underdoping in terms of a midgap pseudo-resonance mode in the Raman intensity.¹⁵ We also found that fermionic damping gives rise to a finite width of the resonance neutron peak.

It is our pleasure to thank G. Blumberg, A. Finkel'stein, D. Morr, and M. Norman for useful conversations. The research was supported by NSF DMR-9629839.

- ¹H.F. Fong *et al.*, Phys. Rev. B **54**, 6708 (1996); P. Dai *et al.*, Science **284**, 1344 (1999).
- ²H.F. Fong *et al.*, Nature (London) **398**, 588 (1999).
- ³G. Blumberg *et al.*, Science **278**, 1427 (1997); J. Phys. Chem. Solids **59**, 2196 (1998).
- ⁴K. Maki and H. Won, Phys. Rev. Lett. **72**, 1785 (1984); D.Z. Liu, Y. Zha, and K. Levin, *ibid.* **75**, 4130 (1995); I. Mazin and V. Yakovenko, *ibid.* **75**, 4134 (1995); A.J. Millis and H. Monien, Phys. Rev. B **54**, 16 172 (1996); N. Bulut and D.J. Scalapino, Phys. Rev. B **53**, 5149 (1996).
- ⁵Z.-X. Shen and J.R. Schrieffer, Phys. Rev. Lett. **78**, 1771 (1997).
- ⁶M.R. Norman and H. Ding, Phys. Rev. B **57**, R11 089 (1998).
- ⁷Ar. Abanov and A. Chubukov, Phys. Rev. Lett. **83**, 1652 (1999).
- ⁸D.K. Morr and D. Pines, Phys. Rev. Lett. **81**, 1086 (1998).
- ⁹A.A. Abrikosov and V.M. Genkin, Zh. Éksp. Teor. Fiz. **65**, 842 (1973) [Sov. Phys. JETP **38**, 417 (1974)].
- ¹⁰M.V. Klein and S.B. Dierker, Phys. Rev. B **29**, 4976 (1984).
- ¹¹B.S. Shastry and B.I. Shraiman, Phys. Rev. Lett. **65**, 1068 (1990); R.R.P. Singh, Comments Condens. Matter Phys. **15**, 241 (1991).
- ¹²T.P. Devereaux and D. Einzel, Phys. Rev. B **51**, 16 336 (1995); H. Won and K. Maki, *ibid.* **49**, 1397 (1994). See also, D. Branch and J.P. Carbotte, *ibid.* **52**, 603 (1995); T. Strohm and M. Cardona, *ibid.* **55**, 12 725 (1997) and references therein.
- ¹³R. Hackl *et al.*, J. Low Temp. Phys. **105**, 733 (1996); R. Nemeschek *et al.*, Phys. Rev. Lett. **78**, 4837 (1997).
- ¹⁴Ch. Renner *et al.*, Phys. Rev. Lett. **80**, 149 (1998).
- ¹⁵A. Chubukov, D. Morr, and G. Blumberg, Solid State Commun. **112**, 183 (1999).
- ¹⁶L.P. Gor'kov, Pis'ma Zh. Éksp. Teor. Fiz. **40**, 351 (1984) [JETP Lett. **40**, 1155 (1984)]; P.J. Hirschfeld, P. Wolfle, and D. Einzel, Phys. Rev. B **37**, 83 (1988); L.S. Borkowski and P.J. Hirschfeld, *ibid.* **49**, 15 404 (1994); A. Zawadowski and M. Cardona, *ibid.* **42**, 8798 (1990); Ye Sun and K. Maki, *ibid.* **51**, 6059 (1995).
- ¹⁷T.P. Devereaux and A.P. Kampf, Int. J. Mod. Phys. B **11**, 2093 (1997); T.P. Devereaux, Phys. Rev. Lett. **74**, 4313 (1995).
- ¹⁸P.A. Lee, Phys. Rev. Lett. **71**, 1887 (1993); A.A. Nersisyan, A.M. Tselik, and F. Wenger, *ibid.* **72**, 2628 (1994); T. Senthil and M.P.A. Fisher, Phys. Rev. B **60**, 6893 (1999).
- ¹⁹J.R. Schrieffer, *Theory of Superconductivity*, Frontiers in Physics (Benjamin/Cummings, Reading, MA, 1964); A. Bardasis and J.R. Schrieffer, Phys. Rev. **121**, 1050 (1961).
- ²⁰H. Monien and A. Zawadowski, Phys. Rev. B **41**, 8798 (1990).
- ²¹A.V. Chubukov and D.K. Morr, Phys. Rev. Lett. **81**, 4716 (1998).
- ²²Ar. Abanov, A. Chubukov, and A. Finkel'stein, cond-mat/9911445 (unpublished).